Study on positive-negative pressure seed metering device for wide-seedling-strip-seeding

Xiaoshun Zhao[1,2*], Wenjie Bai[1], Jincai Li[2], Huali Yu[1], Dawei Zhao[1], Baozhong Yin[3]

(1. *College of Mechanical and Electrical Engineering, Hebei Agricultural University, Baoding 071001, Hebei, China*;
2. *State Key Laboratory of North China Crop Improvement and Regulation, Hebei Agricultural University, Baoding 071001, Hebei, China*;
3. *College of Plant Protection, Hebei Agricultural University, Baoding 071001, Hebei, China*)

Abstract: In order to solve the problem of poor uniformity of wheat strip sowing, this paper designs a positive-negative pressure wheat wide-seedling-strip-seeding precision seed metering device, which adopts the roller structure with the principle of combined positive-negative pressure. Through theoretical analysis and relevant data, the structure of the seed metering device and the structure of the positive-negative pressure air chamber were designed. The internal flow field conditions were simulated by Fluent software under different structural parameters. The design of the seed holes was completed by analyzing the pressure cloud diagram and the flow velocity vector diagram, and the optimal combination of parameters was obtained and the influence law of negative pressure on the flow field was obtained. The effect of rotational speed on the flow field was studied by EDEM-Fluent coupling technique. In this paper, a three-factor and three-level response surface test was conducted on a JPS-12 test bench with Liangxin-99 wheat as the research object. The experiment was conducted with the rotational speed of seed metering device, the negative pressure of seed suction and the seeding height as factors, and the qualified index, the reseeding index and the miss-seeding index as evaluation indicators. Through the test, the optimal structure and working parameters of the seed metering device were determined as follows: the diameter of the seed hole was 2 mm, and the number of seed holes per row was 28, negative pressure was −3.5 kPa, rotational speed of seed metering device was 19 r/min, and seeding height was 180 mm. Validation test was carried out on the optimized seed metering device: the qualified index was 80.62%, the reseeding index was 9.22%, and the miss-seeding index was 10.16%, which reached the parameter indicator in JB/T 10293-2013 Technical conditions of single seed (precision) seeder and met the agronomic requirements for wheat wide-seedling-strip-seeding.

Keywords: wheat, precision, seed metering device, wheat wide-seedling-strip-seeding, positive-negative pressure, fluent, EDEM-Fluent coupling, response surface test

DOI: 10.25165/j.ijabe.20221506.7261

Citation: Zhao X S, Bai W J, Li J C, Yu H L, Zhao D W, Yin B Z. Study on positive-negative pressure seed metering device for wide-seedling-strip-seeding. Int J Agric & Biol Eng, 2022; 15(6): 124–133.

1 Introduction

Wheat is a substantial source of energy throughout the world for human beings[1]. Wheat seeding methods mainly include hole sowing, scatter sowing, and strip sowing. Among them, strip sowing is the most widely used sowing method in China. It is a simplified cultivation technique that saves labor and improves the structure of wheat populations. However, it has the problems of uneven seed distribution per unit area, easy bunching, and uneven development among individuals. To solve these problems, scholars have proposed a variety of wheat sowing techniques, such as narrow seeding, and wide-seedling-strip-seeding[2-4]. Among them, the wheat wide-seedling-strip-seeding technology is a high-yielding cultivation technology proposed by academician Yu et al.[5] It increases the space for individual wheat growth by increasing the width of the seeding and expanding the row spacing. The experimental results showed that the wheat wide-seedling-strip-seeding technology has better germination rate, spike rate, thousand-grain weight, and yield than strip sowing[6].

At present, the models used for wheat wide-seedling-strip-seeding in the market are Shandong 2BJK-6 and Dahua Baolai 2BFJK-8/4, both of which are mechanical slot-wheel seed metering devices. They are simple in structure and low in cost, but they have problems of a high seed-injuring rate and uneven seed distribution[7,8]. Liu et al.[9,10] designed a wheat wide-seedling-strip-seeding precision hook-hole type seed metering device. And to promote uniform sowing of wheat and improve the quality of operation, it used brushes to remove excess seeds from the nests and used rigid cards to force seeds to be cast. Zhai et al.[11] used EDEM software to assist in the design of a wheat wide-seedling-strip-seeding seed metering device. And it used an inclined slotted wheel, a seed guide groove, and a seed guide tube in conjunction to achieve seeding. The above studies are all mechanical seed metering devices, and they have problems such as high seed-injuring rate and poor seed filling performance in high-speed operation.

Received date: 2021-12-13 **Accepted date:** 2022-09-27

Biographies: Wenjie Bai, MS candidate, research interest: agricultural mechanization engineering, Email: 18398263005@163.com; **Jincai Li,** PhD, Professor, research interest: crop cultivation, Email: kjzl@hebau.edu.cn; **Huali Yu,** Master, research interest: vehicle engineering, Email: 48796619@qq.com; **Dawei Zhao,** MS candidate, research interest: agricultural mechanization engineering, Email: david-ok-ok@163.com; **Baozhong Yin,** PhD, Associate Professor, research interest: physiological ecology of crop stress resistance, Email: yinbaozhong@hebau.edu.cn.

***Corresponding author: Xiaoshun Zhao,** PhD, Associate Professor, research interest: modern agricultural equipment design and control, precision planting technology. College of Mechanical and Electrical Engineering, Hebei Agricultural University, Baoding 071001, Hebei, China. Tel: +86-17330263721, Email: zhao_xsh@126.com.

With the promotion of precision seeding technology, the pneumatic seed metering devices have gradually replaced the mechanical seed metering devices, and will be the mainstream of future development[12,13]. The foreign air-suction precision seed metering devices are mainly used for precision sowing of cultivated crops, such as maize[14]. Wheat sowing is dominated by a mechanical seed metering device and supplemented by a pneumatic seed metering device[15-18]. Wheat sowing in China mainly uses mechanical seed metering devices, and single grain precision pneumatic wheat seed metering devices have been studied more in recent years, but they are still in the laboratory stage[19,20]. Zhao et al.[21,22] designed a pneumatic seed metering device to realize the precision sowing of wheat and millet. Cheng et al.[23] designed a wheat precision seed metering device with a combination of pneumatic and type holes. They optimized the parameters through simulation and bench tests to obtain good single grain seed filling performance. All of the above seed metering devices rely on the gravity of the seeds themselves to complete seeding, but since wheat seeds are small and cannot be completely dispersed by gravity. So, the positive-negative pressure seed metering devices have been developed. Liu et al.[24] conducted a theoretical analysis of the structure of a pinhole-tube wheat precision seed metering device. And they conducted an orthogonal test using Fluent software to optimize the seeding performance. Liao et al.[25-27] designed and tested a pneumatic rape precision seed metering device, and they solved the problems of clogging and miss-seeding.

Based on the above research, this paper uses the combination of positive-negative pressure to design a wheat wide-seedling-strip-seeding seed metering device. It is used to match the agronomic technology of wheat wide-seedling-strip-seeding seed metering device. Meanwhile it is important to improve the uniformity of wheat sowing, save seeds, reduce the seed-injuring rate and improve the operation efficiency.

2 Materials and methods

2.1 Structure of seed metering device

The seed metering device is mainly composed of roller, positive pressure chamber, negative pressure chamber, central tube shaft, seed box, transmission gear, cover, bearing and bearing chock, as shown in Figures 1 and 2. The central tube shaft of seed metering device is connected to the fan through a hose, and the positive-negative pressure are provided by the positive pressure inlet hole and the negative pressure suction hole respectively. The positive-negative pressure central tube shaft adopts the form of single shaft to ensure the coaxiality of the seed metering device. According to the literatures[28-31] and practical experience, the basic structural parameters of the seed metering device were determined: the outer diameter of the roller was 180 mm, and the outer diameter of the central tube shaft was 25 mm. According to the agronomic requirements of wheat wide-seedling-strip-seeding, 5 rows of seed holes were distributed on the roller, and the spacing between adjacent holes was 20 mm.

2.2 Air chamber design

As shown in Figure 3, the negative pressure chamber is located directly above the inner roller, accounting for 300 ° of the inner roller arcs, and the central area is a circle with a wide area in the middle and a gradually narrowing area on both sides, so that the negative pressure chamber has higher air pressure on both sides and slightly lower air pressure in the central area, ensuring reliable adsorption of wheat seed.

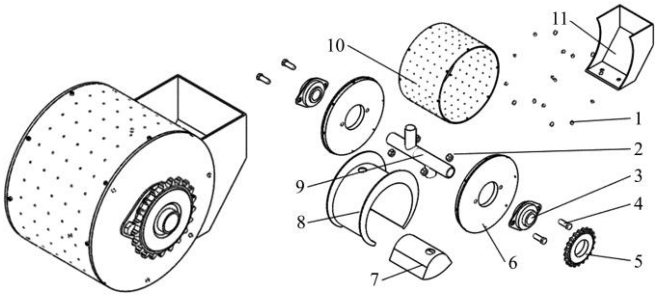

a. Whole structure of the device b. Exploded view of the whole assembly structure

1. Top screw 2. Nut 3. Bearing and bearing seat 4. Bolt 5. Transmission gear 6. End cover 7. Positive pressure chamber 8. Negative pressure chamber 9. Central tube shaft 10. Roller 11. Seed box

Figure 1 Normal distribution diagram of the three-axis

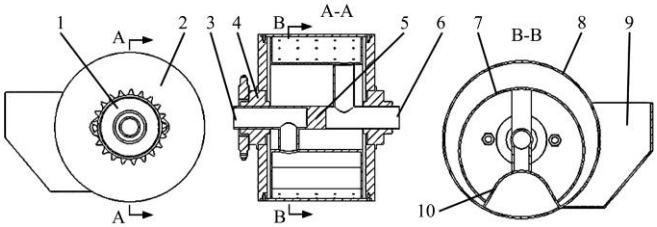

1. Transmission gear 2. End cover 3. Positive pressure inlet opening 4. Bearing and bearing seat 5. Central tube shaft 6. Negative pressure suction opening 7. Negative pressure chamber 8. Roller 9. Seed box 10. Positive pressure chamber

Figure 2 Sectional view of seed metering device

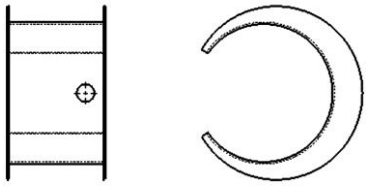

Figure 3 Structure diagram of negative pressure chamber

As shown in Figure 4, the positive pressure chamber is located directly below the inner drum, accounting for 60 °of the inner roller arcs, and is used to assist in seeding and cleaning.

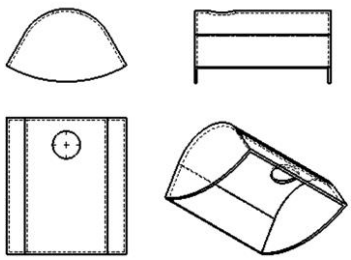

Figure 4 Structure diagram of positive pressure chamber

2.3 Seed hole design

According to Equation (1), under the condition of certain fan power, decreasing the diameter of the seed hole will lead to insufficient adsorption force of the roller and the phenomenon of missed seeding, increasing the diameter will lead to too strong adsorption capacity and the phenomenon of repeat sowing. Considering the difference in the three-dimensional dimensions of wheat seeds, five different sizes of 1.6, 1.8, 2.0, 2.2, and 2.4 mm were selected for simulation analysis according to Equation (2) to determine the seed hole diameters. The number of seed holes also affects the seed absorption capacity of the roller. Five parameters, 14, 21, 28, 35, and 42, were selected for simulation tests to determine the number of seed holes according to the agronomic requirements.

$$P = \frac{\pi d^2}{4}(P_0 - P_1) \quad (1)$$

$$d = (0.64 \sim 0.66)b \quad (2)$$

2.4 Principle of operation

As shown in Figure 5, according to the force and distribution of wheat seeds, the outer circle of the roller is divided into 3 regions: unstable region, stable region and falling region. The unstable region is covered by wheat seeds. In this region, the seeds close to the outer edge of the roller are in a changing state of motion due to the influence of negative pressure suction, surface friction of roller, gravity, friction between seeds and seeds and extrusion force. In the stable region, the wheat is in a stable state under the action of negative pressure suction and its gravity. The adsorbed wheat seeds are separated from the seed population with the clockwise movement of the roller, and after passing through the stable region, they enter the seeding region. In the seeding region, the wheat seed is released from the seed hole by its gravity and positive pressure blowing force and falls into the seed trench.

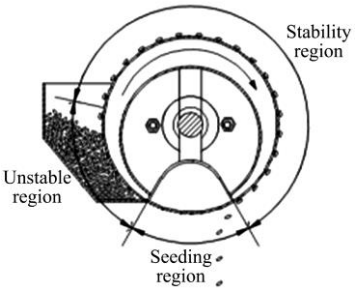

Figure 5 Structure of the seed metering device

2.5 Model processing

The three-dimensional model of seed metering device with different structural parameters was established by SolidWorks software. As shown in Figure 6, the model is imported into Space Claim 2019 R3 for volume extraction and building the flow field model. According to the characteristics of flow field distribution, the simulation model was divided into three main regions: negative pressure region, positive pressure region, and seed hole region. The flow field model was imported into Fluent 2019 R3 software and meshed in a tetrahedral manner. Local dimensional encryption was performed at the seed holes, and five layers of expansion layer mesh were generated at the near-wall surface. After the overall mesh is generated, the mesh quality was checked and adjusted, and it was found that the overall maximum deviation was less than 0.9, which was good. The divided meshes are shown in Figure 7 and Figure 8.

2.6 Boundary condition setting

The finite volume method was used to establish the discrete equations, and the pressure-based solver was selected for the steady-state solution. The turbulence model was chosen as the standard k-ε model, and the near-wall region is set as a standard wall surface. The material is set to air, the solution is performed at room temperature, and other terms are kept as default settings.

The end face of the seed hole connected with atmospheric pressure was defined as a pressure outlet, and the pressure was set to 0 kPa. The two-port types of the central tube shaft were set as pressure inlet, the pressure connected to the positive pressure area was set to 0.3 kPa, and the port pressure connected to the negative pressure region was set as −2.0, −2.5, −3.0, −3.5, and −4.0 kPa, respectively. There were two interfaces in the model, and the other items remain default.

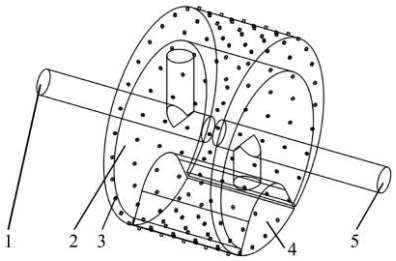

1. Negative pressure suction opening 2. Negative pressure area 3. Seed hole area 4. Positive pressure area 5. Positive pressure inlet opening

Figure 6 Flow field model inside the seed metering device

Figure 7 Grid of the seed metering device

Figure 8 Flow field grid profile

After 500 steps of the iterative calculation, the consumption rates of momentum, k turbulent kinetic energy, and ε turbulent kinetic energy in three directions were all less than 1×10^{-3}, and the continuity was less than 3×10^{-2}. By calculating the fluid masses of all inlets and outlets, the calculation is judged to converge when the mass difference was less than 0.5%. The residual plot is shown in Figure 9.

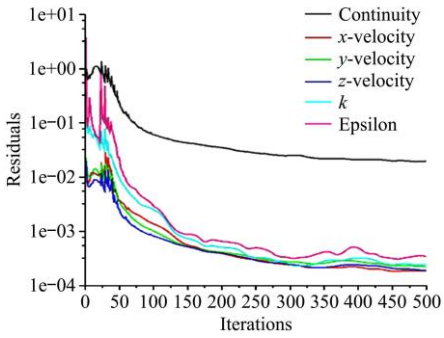

Figure 9 Residual plot at 500 iterations

2.7 EDEM-Fluent coupling parameter setting

The seed metering device model in stl format was imported into EDEM, the model material was set to 304 stainless steel, and the analytical model is shown in Figure 10. The simplified model of particles is shown in Figure 11. The size distribution was set to a normal distribution and the number is 4000 particles. The model parameters in EDEM are shown in Table 1, the physical contact model was set to Hertz-Mindlin (no-slip) model, the particle plant was set at the opening of the seed box, the gravitational acceleration is set to 9.81 m/s^2, the direction was along the negative direction of Y axis, the initial drop velocity was set to 2 m/s, and the time duration in EDEM was set to about 28% of the Rayleigh time step (5×10^{-5} s).

After the first simulation of EDEM, wheat grains need to fall into the seed box first and deposit naturally under the action of gravity, and the simulation time was 5 s. In the second simulation, the drum was set to rotate at 15, 19, 23, 27, and 31 r/min respectively, and the simulation time was 5 s.

After the first simulation of EDEM was finished, the export settings are performed as shown in Figure 12, and the coupling interface was started at the beginning of the second simulation, followed by the settings in Fluent. The settings in fluent were set to the transient solution, the negative pressure port was set to −3.5 kPa, the positive pressure port was set to 0.3 kPa, the rotational speed in the seed hole region was synchronized with that in EDEM, and the sub-relaxation factor was adjusted appropriately, the coupling UDF file is loaded (as shown in Figure 13), the time step was set to an integer multiple of the EDEM time step (1×10^{-3} s), the number of steps was set to 5000, and the rest items kept the default.

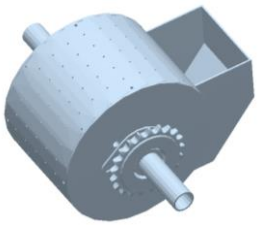

Figure 10 EDEM analysis model

Figure 11 Wheat particle model

Table 1 Material mechanical properties and interaction parameters

Material parameter				Exposure parameter			
Material	Shear modulus/Pa	Density/kg·m^{-3}	Poisson ratio	Contact material	Coefficient of restitution	Coefficient of static friction	Coefficient of kinetic friction
Wheat	2.6×10^{6}	1350	0.3	Wheat-wheat	0.2	1.0	0.01
Stainless steel	7.938×10^{10}	7900	0.3	Wheat-stainless steel	0.5	0.5	0.01

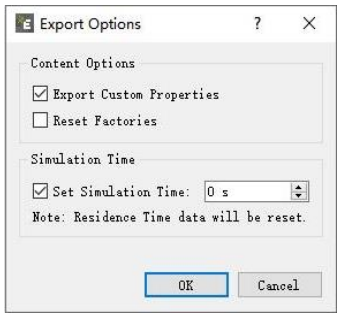

Figure 12 EDEM export settings

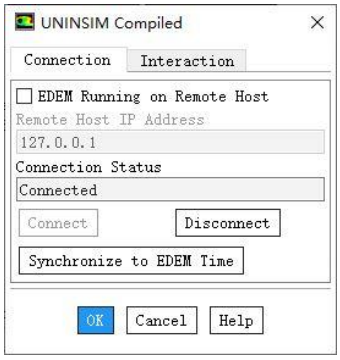

Figure 13 Coupling interface settings

2.8 Working performance test

Liangxin-99 was used as the research object, its average length was 6.29 mm, the average width was 3.39 mm, the average thickness was 3.11 mm, the thousand seed weight was 39.6 g, and the purity was 98%, and the seeds were not graded. The physical seed metering device is shown in Figure 14, and the test bench is shown in Figure 15.

In the experiment, the data were recorded when the rotational speed of the seed metering device was stable, and every 10 weeks of the roller was a cycle. With the help of computer image processing technology, the test data were counted. The recognition width corresponding to each row of seed holes was 20 mm (according to the row spacing of seed holes). The relationship between the seed bed belt speed and the rotational speed of the seed metering device is shown in Equation (3), according to the agronomic requirement, the grain spacing is 20 mm, and the theoretical grain spacing is constant in the experiment.

$$l=\frac{60v_1}{v_2 n} \tag{3}$$

where, n is the number of single row holes in the circumferential direction of the roller; v_1 is the speed of seed bed belt, m/s; l is the theoretical distance, m; v_2 is the rotational speed of seed metering device, r/min.

The test was conducted with the qualified index of seed spacing, reseeding index, and miss-seeding index as the evaluation indicators, the test method and requirements for indicators were carried out according to the standards GB/T 6973-2005 and JB/T 10293-2013. Each group of tests was repeated three times, and the average value was taken as the result.

Figure 14 Picture of the seed metering device

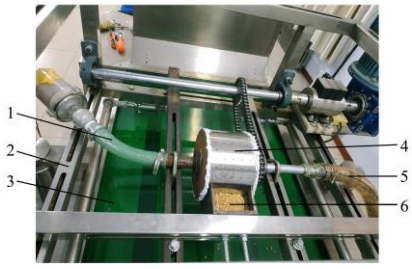

1. Positive pressure air supply pipe 2. Seed metering device holder 3. Seed bed belt 4. Roller 5. Negative pressure air supply pipe 6. Seed box

Figure 15 Test device of the seed metering device

3 Results and discussion

3.1 Seed hole design based on simulation

To express the pressure and velocity distribution of the flow field inside the seed hole, the pressure cloud diagram of the radial section and velocity vector diagram of the five rows of seed holes in the seed metering device were established respectively. When the negative pressure is −2 kPa, the pressure cloud diagram and velocity vector diagram of each row section are shown in Figures 16 and 17. The pressure cloud diagram of the flow field in the negative pressure region and its contact hole is shown in Figure 18.

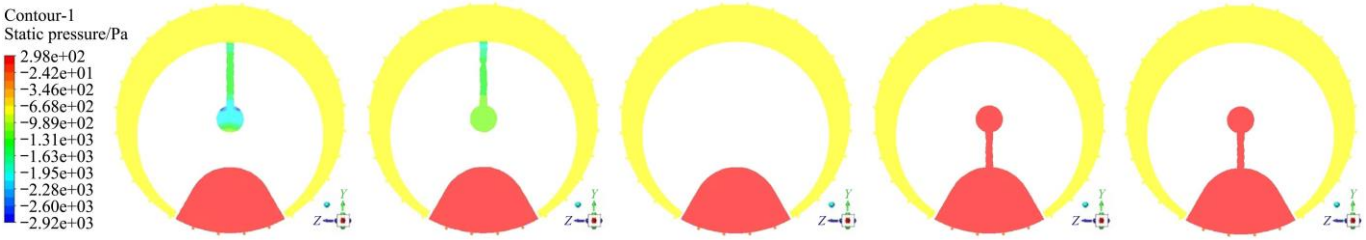

a. Row 1 b. Row 2 c. Row 3 d. Row 4 e. Row 5

Figure 16 Pressure nephogram of each section

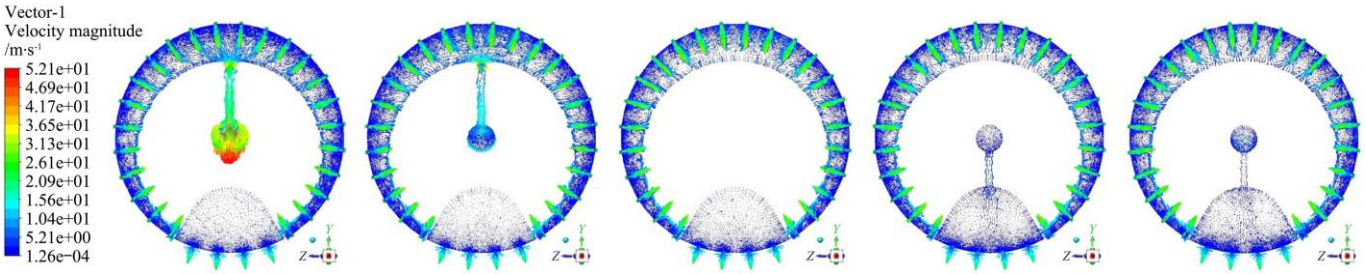

a. Row 1 b. Row 2 c. Row 3 d. Row 4 e. Row 5

Figure 17 Velocity vectogram of each section

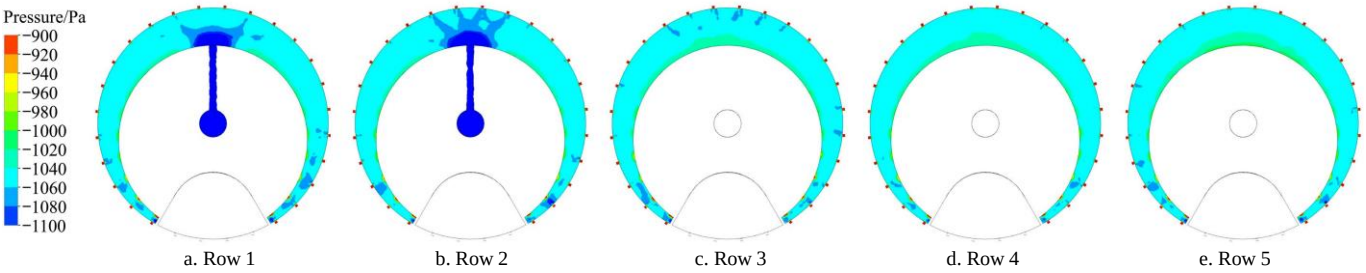

a. Row 1 b. Row 2 c. Row 3 d. Row 4 e. Row 5

Figure 18 Pressure nephogram of negative pressure area

It can be seen from Figures 16-18 that the difference of flow field state in each row hole of roller is small. In a single section, there is no obvious difference in the flow field state in the seed hole contacted with the negative pressure region. When the parameters of the seed metering device are changed, the analysis should focus on the flow field in the seed holes in contact with the negative pressure region to determine the adsorption capacity of the seed holes. Therefore, in the following analysis of the flow field, only the changes of the flow field in the diameter-oriented cross-section of the seed holes in the middle row of the roller was analyzed[32].

The flow field inside the seed metering device was simulated and analyzed with the seed hole diameter as the variable to simulate the variation of the flow field at different levels. Five different seed hole diameters of 1.6, 1.8, 2.0, 2.2, and 2.4 mm were tested with a negative pressure value of −3.0 kPa and a number of 28 seed holes. The pressure cloud diagram and velocity vector diagram of radial section are shown in Figure 19 and Figure 20.

According to the parameter values of the flow field in the seed hole, the point-line diagram (Figure 21) shows that the absolute pressure and velocity of the flow field in the seed hole increase and then decrease as the diameter of the seed hole becomes larger, and the changes are obvious. The pressure and velocity of the flow field in each seed hole do not change much and are relatively stable.

As shown in Figure 19, the flow field changes significantly when the orifice diameter is 1.8 mm and 2.0 mm, and the pressure distribution is similar in other orifice diameters. As can be seen from Figure 20, the flow velocity is larger in the case of orifice diameter of 1.8 mm and 2.0 mm. By comparing Figure 19b and Figure 19c, the air pressure distribution in Figure 19b is more uniform, but the change of pressure gradient in its seed filling area is not obvious. Considering that the appropriate pressure gradient change in the filling area will cause certain disturbance to the seed, and it can improve the filling performance. So, the seed hole diameter was designed to be 2.0 mm.

The simulation analysis was carried out with the number of seed holes as the variable, 14, 21, 28, 35, and 42, respectively, to simulate the variation of the flow field at five levels. Under the conditions of 2.0 mm seed hole diameter and −3.0 kPa negative pressure, the pressure cloud diagrams and velocity vector diagrams of the radial section with the different number of seed holes are shown in Figures 22 and 23, respectively.

The point-line diagram (Figure 24) based on the flow field parameters in the seed hole shows that with the increase of the number of seed holes, the absolute value of pressure and velocity of the flow field in the seed holes change obviously and decrease rapidly.

It can be seen from Figure 22 that the pressure distribution of

the flow field is more similar when the number of seed holes is 14 and 21, and its distribution is more uniform, but there is no obvious pressure gradient change in the seed filling area. When the number of holes is more than 28, the flow field has obvious pressure gradient classification. With the increase of the number of holes, the negative pressure and velocity of the flow field decrease gradually. Therefore, considering the filling performance and fan energy consumption, the number of seed holes was set to 28.

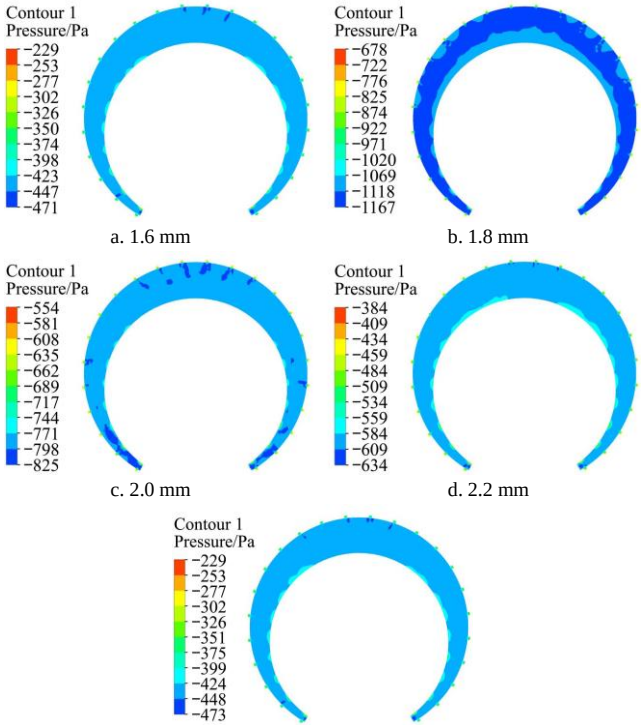

Figure 19 Pressure nephogram under different seed-suction hole diameters

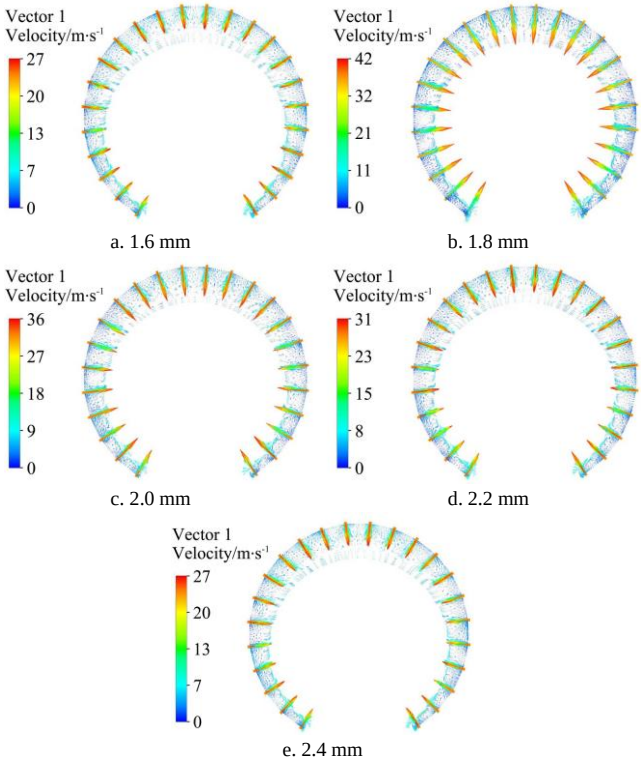

Figure 20 Velocity vectogram under different seed-suction holes diameter

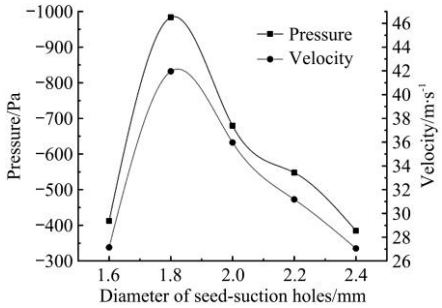

Figure 21 The effect of seed-suction hole diameter on the flow field in seed-suction holes

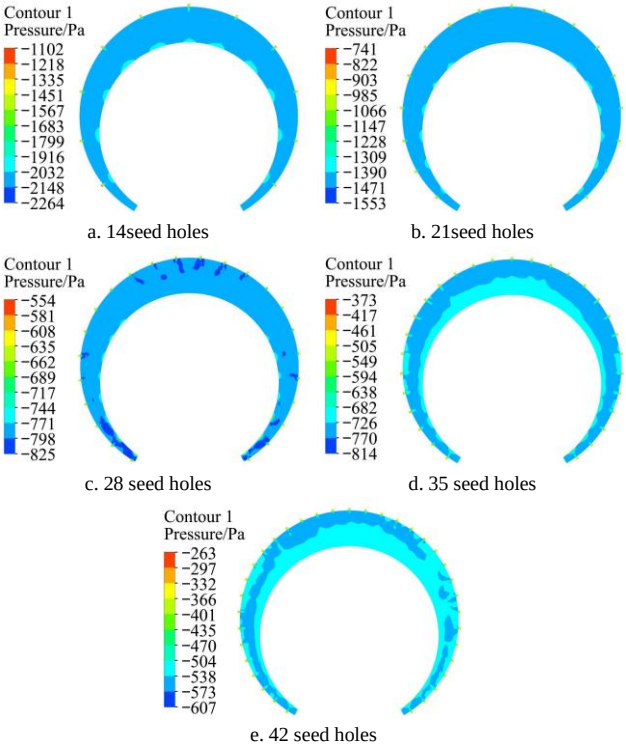

Figure 22 Pressure nephogram under different number of holes

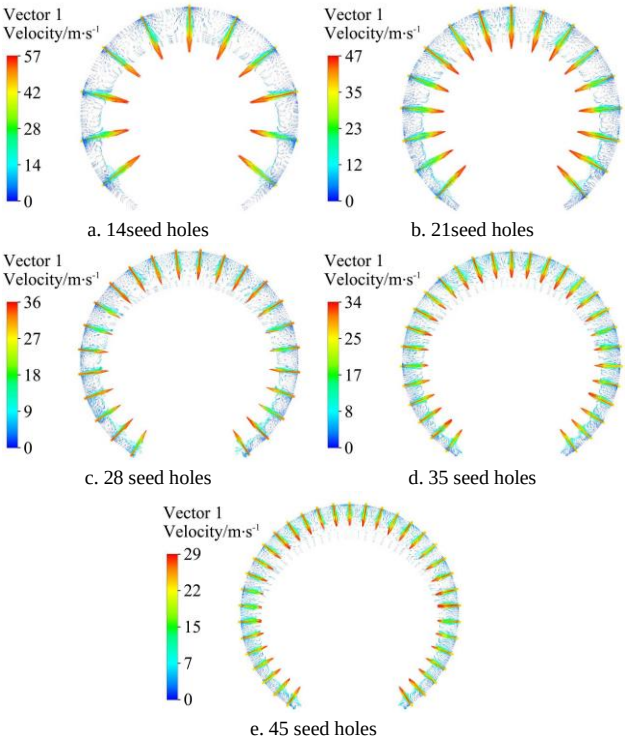

Figure 23 Velocity vectogram under different number of holes

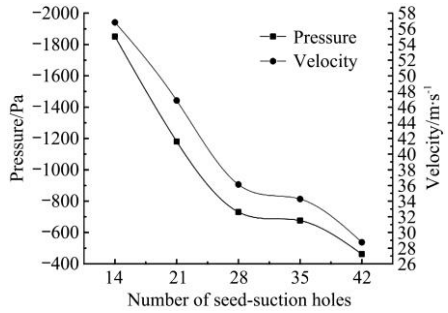

Figure 24 The effect of the number of seed-suction holes on the flow field in the seed-suction holes

3.2 Determination of suction negative pressure

Simulation analysis was carried out with the suction negative pressure value as a variable, the negative pressure of suction was set to −2.0, −2.5, −3.0, −3.5, and −4.0 kPa. The diameter of seed holes was 2.0 mm, and the number of seed holes was 28. The flow field states under different pressures are shown in Figure 25 and Figure 26.

According to the line chart (Figure 27), the pressure and velocity inside the air chamber increased with the increase of the suction negative pressure. However, considering the power consumption of the fan and the reseeding problem caused by the excessive negative pressure, the negative pressure is not the greater the better.

It can be seen from Figure 25 that the pressure distribution is more uniform when the negative pressure is 4.0 kPa, but there is no obvious pressure gradient change in the seed filling area, which is not conducive to seed filling. Under other negative pressure conditions, the flow field distribution in the chamber is similar. However, compared with the flow field distribution under the condition of − 2.5 to − 3.5 kPa, the flow field change in the stable region with negative pressure of − 2.0 kPa is more complicated, and the stability of seed movement is poor. Therefore, follow-up to −2.5 to −3.5 kPa negative pressure range test to determine the size of the suction negative pressure.

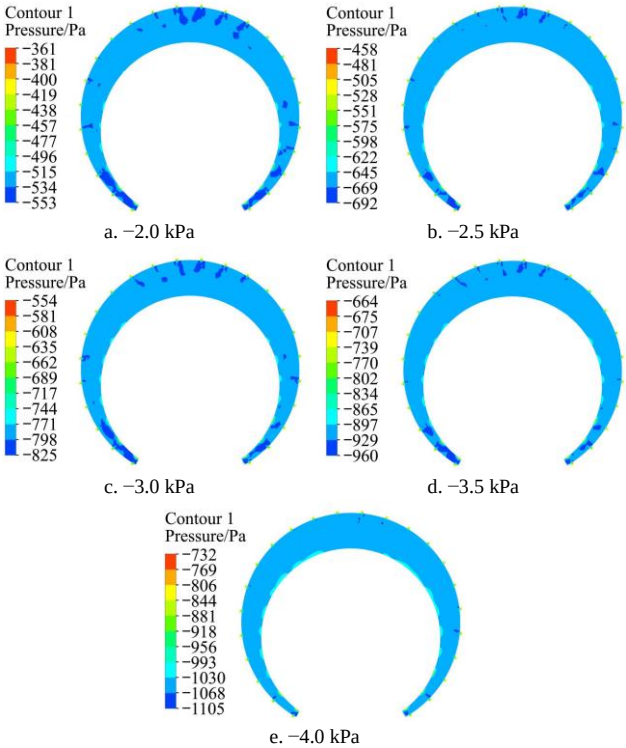

Figure 25 Pressure nephogram under different negative pressure

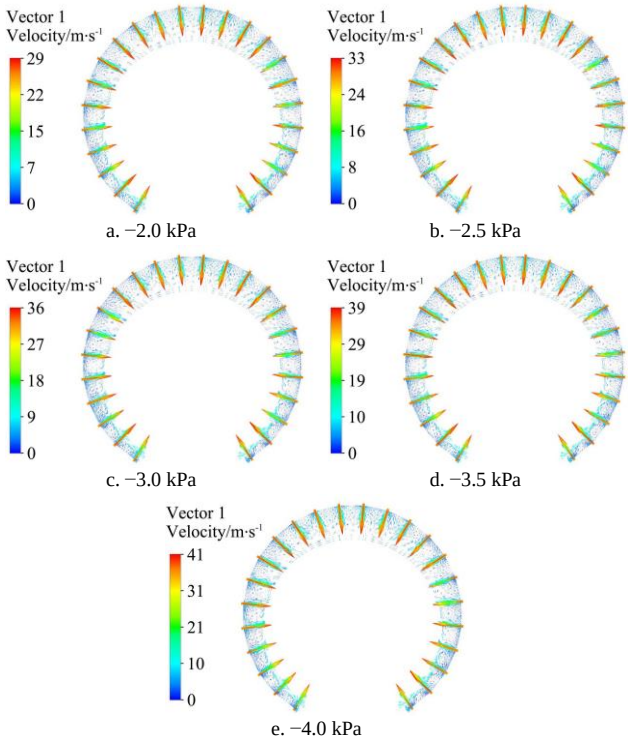

Figure 26 Velocity vectogram under different negative pressure

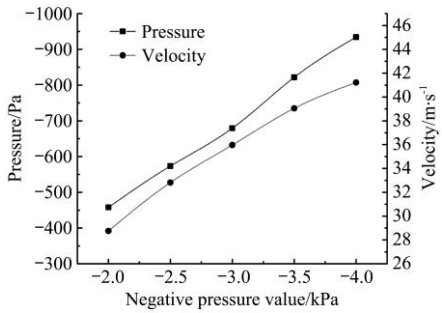

Figure 27 Effect of negative pressure on the flow field in the seed-suction holes

3.3 Determination of roller speed

The seed holes were counted when they were rotated to the highest point of the seed metering device. Adsorption of one seed is defined as qualified, adsorption of two or more seeds is defined as reseeding, and non-absorbed seeds are defined as miss-seeding. After each change of the simulation parameters, the adsorption of 100 seed holes was counted. The movement path of a single seed is shown in Figure 28, which is consistent with the actual movement trend and illustrates the reliability of the simulation.

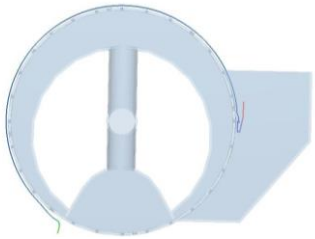

Figure 28 Motion trajectory diagram of single seed

The qualified rate, miss-seeding rate, and reseeding rate at five levels were counted as shown in Table 2. From Figure 28, it can be seen that the qualified rate increases and then decreases as the rotational speed increases, and the reseeding rate and miss-seeding rate decrease and then increase. At the same time, the qualified rate was better at 15-27 r/min, all of which were greater than 80%,

but the reseeding rate was higher at 15 r/min, so the better rotational speed of the seed metering device was 19-27 r/min.

Table 2 Speed level and test results of seed-metering device

Rotational speed/r·min^{-1}	Qualified index /%	Reseeding index /%	Miss-seeding index/%
15	61.19	28.32	10.49
19	68.35	24.06	7.59
23	72.96	13.91	13.13
27	75.38	8.78	15.84
31	65.66	6.95	27.39

3.4 Single-factor test

According to multiple tests and the negative pressure range provided by the fan, the range of negative pressure was set from −1.5 to −3.5 kPa, the range of rotational speed was set from 15 to 31 r/min, and the range of seeding height was set from 100 to 250 mm. Each level was repeated three times, and the test results are listed in Table 3.

Table 3 Single factor experimental results

Factors	Values	Qualified index y_1/%	Reseeding index y_2/%	Miss-seeding index y_2/%
Negative pressure x_1/kPa	−1.5	42.29	6.78	50.93
	−2.0	51.64	9.91	38.45
	−2.5	64.41	10.25	25.34
	−3.0	72.96	13.91	13.13
	−3.5	67.34	21.72	10.94
Rotational speed of seed metering device x_2/r min^{-1}	15	61.19	28.32	10.49
	19	68.35	24.06	7.59
	23	72.96	13.91	13.13
	27	75.38	8.78	15.84
	31	65.66	6.95	27.39
Seeding height x_3/mm	100	72.96	13.91	13.13
	150	68.51	17.06	14.43
	200	65.95	22.78	11.27
	250	66.01	12.37	21.62

3.5 Response surface testing

A three-factors and three-level response surface test was designed with negative pressure, rotational speed of seed metering device and seeding height as factors. The significance of each factor on the test index was obtained by regression equation and analysis of variance. The range of test factors was determined according to the single-factor test results, and the test was designed using the Box-B Behnken response method of Design-Expert software. The test factor levels are shown in Table 4, and the design scheme is shown in Table 5 (X_1, X_2, and X_3 respectively represent the coded values of negative pressure, rotational speed of seed metering device and seeding height).

Multiple regression fitting analysis and variance analysis were performed on the test results in Table 5, and the results are shown in Tables 6, 7, and 8. The quadratic regression fitting equations for the qualified rate and the linear regression fitting equations for the reseeding rate and the miss-seeding rate were obtained, as shown in Equations (4)-(6). In the variance analysis, the *p*-values of the three models were less than 0.05, and the *p*-values of the three mismatch items were greater than 0.05, indicating that the regression equations were credible and could fit the real test results.

$$y_1=54.8-0.72x_1-11.17x_2+2.29x_3-3.03x_1x_2+4.25x_1x_3+1.92x_2x_3+0.18x_1^2+1.38x_2^2+7.95x_3^2 \quad (4)$$

$$y_2=14.15+5.06x_1+2.91x_2-2.09x_3 \quad (5)$$

$$y_3=26.56-4.36x_1+8.28x_2-0.22x_3 \quad (6)$$

From the variance analysis of the y_1 model (the qualified index), X_2 had a highly significant impact on y_1, X_3^2 had a significant impact on y_1, and other factors did not have a significant impact on the model. From the variance analysis of the y_2 model (the reseeding index), X_1 had a highly significant impact on y_2, and other factors did not have a significant impact on the model. From the analysis of variance of the y_3 model (the miss-seeding index), X_2 had a highly significant impact on y_3, X_1 had a significant effect on y_3, and other factors did not have a significant effect on the model.

It could be seen from the test results that the factors affecting the working performance of the seed metering device were mutually restricted. The main factors affecting the qualified index were the rotational speed of the seed metering device and the seeding height. The main factors affecting the reseeding index were negative pressure, and the main factors affecting the miss-seeding index were the negative pressure and the rotational speed of the seed metering device.

Table 4 Experimental factors and levels

Levels	Negative pressure x_1/kPa	Rotational speed of seed metering device x_2/r min^{-1}	Seeding height x_3/mm
−1	−2.5	19	100
0	−3.0	23	140
1	−3.5	27	180

Table 5 Experimental design and results

No.	X_1	X_2	X_3	Qualified index y_1/%	Reseeding index y_2/%	Miss-seeding index y_3/%
1	0	0	0	46.18	19.41	34.41
2	0	0	0	57.85	20.31	21.85
3	0	1	1	58.70	10.39	30.91
4	0	−1	1	75.78	12.25	11.79
5	1	0	1	69.48	11.63	18.90
6	0	−1	−1	73.41	12.99	13.60
7	0	0	0	52.84	18.51	28.66
8	−1	0	1	59.33	5.22	35.45
9	−1	0	−1	64.89	7.21	27.90
10	1	−1	0	69.01	10.42	20.56
11	1	1	0	39.18	29.47	31.25
12	0	0	0	56.36	17.92	25.72
13	0	0	0	60.76	11.34	27.91
14	−1	1	0	49.78	9.69	40.53
15	1	0	−1	58.04	18.88	23.08
16	−1	−1	0	67.48	7.77	24.76
17	0	1	−1	48.63	17.12	34.25

Table 6 Variance analysis of the qualified index

Source	Sum of squares	df	Mean square	*F*-value	*p*-value
Model	1450.81	9	161.20	7.33	0.0078**
X_1	4.16	1	4.16	0.19	0.6766
X_2	998.82	1	998.82	45.42	0.0003**
X_3	41.95	1	41.95	1.91	0.2097
X_1X_2	36.78	1	36.78	1.67	0.2369
X_1X_3	72.25	1	72.25	3.29	0.1128
X_2X_3	14.82	1	14.82	0.67	0.4387
X_1^2	0.14	1	0.14	0.01	0.9378
X_2^2	8.02	1	8.02	0.36	0.5651
X_3^2	266.27	1	266.27	12.11	0.0103*
Residual	153.93	7	21.99		
Lack of fit	28.52	3	9.51	0.30	0.8227
Pure error	125.40	4	31.35		
Cor total	1604.74	16			

Note: * means the difference is significant (p<0.05); ** means the difference is highly significant (p<0.01). df means the degree of freedom. The same as below.

Table 7 Variance analysis of the replay-sowing index

Source	Sum of squares	df	Mean square	*F*-value	*P*-value
Model	307.55	3	102.52	4.55	0.0217*
X_1	205.13	1	205.13	9.10	0.0099**
X_2	67.51	1	67.51	3.00	0.1071
X_3	34.90	1	34.90	1.55	0.2353
Residual	292.94	13	22.53		
Lack of fit	242.25	9	26.92	2.12	0.2435
Pure error	50.69	4	12.67		
Cor total	600.49	16			

Table 8 Variance analysis of the leak-sowing index

Source	Sum of squares	df	Mean square	*F*-value	*p*-value
Model	700.51	3	233.50	11.57	0.0006**
X_1	151.82	1	151.82	7.52	0.0168*
X_2	548.30	1	548.30	27.16	0.0002**
X_3	0.40	1	0.40	0.02	0.8907
Residual	262.42	13	20.19		
Lack of fit	178.28	9	19.81	0.94	0.5710
Pure error	84.13	4	21.03		
Cor total	962.93	16			

3.6 Parameter optimization and validation tests

This test focuses on considering the qualified index. And the regression equation of the above three test indexes was solved by constrained objective optimization. The following functions were obtained by optimization:

$$\begin{cases} \max y_1(x_1, x_2, x_3) \\ y_2(x_1, x_2, x_3) < 30\% \\ y_3(x_1, x_2, x_3) < 15\% \\ s.t. \begin{cases} -3.5 < x_1 < -2.5 \\ 19 < x_2 < 27 \\ 100 < x_3 < 180 \end{cases} \end{cases} \quad (7)$$

After numerical optimization, the optimized parameter combinations and predicted value were obtained as follows: negative pressure was −3.5 kPa, rotational speed of seed metering device was 19 r / min, and seeding height was 180 mm.

According to the optimized parameters of the bench test, the test results were as follows: the qualified index was 80.62%, the reseeding index was 9.22%, and the miss-seeding index was 10.16%. And these parameters meet the industry-standard JB/T 10293-2013 Technical conditions of single-seed (precision) seeder indicators: qualified index ≥60%, reseeding index ≤30%, miss-seeding index ≤15%.

4 Conclusions

(1) In order to match the agronomic technology of wheat wide-seedling-strip-seeding, a precision seed metering device was designed based on the principle of positive-negative pressure combination, and the positive-negative pressure air chamber and the seed discharger roller were designed by theoretical analysis.

(2) The fluent simulation was applied to determine the parameters of the seed holes, and the optimal structural parameters of the seed row were obtained: the diameter of the seed holes was 2 mm, the number of seed holes per row was 28, and the effect of negative pressure on the flow field pattern was obtained to assist the completion of the subsequent experiments.

(3) The single factor test and response surface test were carried out on the JPS-12 test bench. The influences of negative pressure, rotational speed of seed metering device and seeding height on the working performance of the seed metering device were obtained by variance analysis. The optimized combination of working parameters was as follows: negative pressure was −3.5 kPa, rotational speed was 19 r/min, and seeding height was 180 mm. At this time, the qualified index of seed spacing was 80.62%, the reseeding index was 9.22%, and the miss-seeding index was 10.16%, which met the technical indicators of JB/T 10293-2013 Technical conditions of single-seed (precision) seeder and the agronomic technical requirements of wheat wide-seedling-strip-seeding.

Acknowledgements

The study was financially supported by State Key Laboratory of North China Crop Improvement and Regulation; Key R&D Projects in Hebei Province (Grant No. 21327215D); Funding Projects for the Returned Overseas Chinese Scholars in 2020, China (Grant No. C20200337).

[References]

[1] Li Y M, Chandio F A, Ma Z, Lakhiar I A, Sahito A R, Ahmad F, et al. Mechanical strength of wheat grain varieties influenced by moisture content and loading rate. Int J Agric & Biol Eng, 2018; 11(4): 52–57.

[2] Jin M F, Ding Y Q, Yu H, Liu H T, Jiang Y Z, Fu X Q. Optimal structure design and performance tests of seed metering device with fluted rollers for precision wheat seeding machine. IFAC-PapersOnLine, 2018; 51(17): 509–514.

[3] Xu G, He R, Li X, Zou Y J, Shi L, Liu T. Design and evaluation of a half-precision sowing and fertilizing combined machine. Journal of Computational and Theoretical Nanoscience, 2016; 13(11): 8081–8087.

[4] Hu H N, Lu C Y, Wang Q J, Li H W, He J, Xu D J, et al. Influences of wide-narrow seeding on soil properties and winter wheat yields under conservation tillage in North China Plain. Int J Agric & Biol Eng, 2018; 11(4): 74–80.

[5] Yu S L. Theory and practice of wheat cultivation in China. Shanghai Science and Technology Press, 2006.

[6] Shi Y H, Chu J P, Yin L J, Deng S Z, Zhang L, Sun X L, et al. Wide-range sowing improving yield and nitrogen use efficiency of wheat sown at different dates. Transactions of the CSAE, 2018; 34(17): 127–133.

[7] Zhu Q Z, Wu G W, Chen L P, Zhao C J, Meng Z J, Shi J T, N. Structural design and optimization of seed separated plate of wheat wide-boundary sowing device. Transactions of the CSAE, 2019; 35(1): 1–11. (in Chinese)

[8] Meng F Y, Zhou J H, Wang J Y, Mao S S, Man J, Tong G X, et al. Study on suitable row spacing of 2BJK-8 wheat wide precision seeder in Beijing. Bulletin of Agricultural Science and Technology, 2015; 4: 88–90.

[9] Liu C L, Wei D, Dou X, Jiang M, Song J N, Zhang F Y. Design and test of wide seedling strip wheat precision hook-hole type seed-metering device. Transactions of the CSAE, 2019; 50(1): 75–84. (in Chinese)

[10] Li H C, Gao F, Niu H H, Chang F. Design and experiment of wide-seedling and hook-shaped hole-wheel precision metering device for wheat. Hubei Agricultural Mechanization, 2019; 22: 171–172. (in Chinese)

[11] Zhai M M. Optimum design and test of wheat wide precision seeding device based on EDEM. Tai'an: Shandong Agricultural University, 2018. (in Chinese)

[12] Lei X L, Hu H J, Yang W H, Liu L Y, Liao Q X, Ren W J. Seeding performance of air-assisted centralized seed-metering device for rapeseed. Int J Agric & Biol Eng, 2021; 14(5): 79–87.

[13] He X, Wang Z M, Luo X W, Zang Y, He S Y, Xu P, et al. Design and experimental analysis of rice pneumatic seeder with adjustable seeding rate. Int J Agric & Biol Eng, 2021; 14(4): 113–122.

[14] Liu K, Yi S J. Design and experiment of seeding performance monitoring system for suction corn planter. Int J Agric & Biol Eng, 2019; 12(4): 97–103.

[15] Geng D Y, Li Y H, Meng P X, Du R C, Meng F H. Design and test on telescopic clip finger type of metering device. Transactions of the CSAE, 2016; 47(5): 38–45. (in Chinese)

[16] Chen L Q, Xie B B, Li Z D, Yang L, Chen Y X. Design of maize precision metering control system based on double closed loop PID fuzzy algorithm. Agricultural Engineering, 2018; 34(9): 33–41.

[17] Wang Y. The experimental study of the wheat precision metering device. Urumqi: Xinjiang Agricultural University, 2006; 67p. (in Chinese)

[18] Qi B, Zhang D X, Liu Q, W Yang L, Si S, Cui T. Design and experiment of cleaning performance in a centralized pneumatic metering device for maize. Transactions of the CSAE, 2015; 31(01): 20–27. (in Chinese)
[19] Liu L J, Yang H, Ma S C. Experimental study on performance of pneumatic seeding system. Int J Agric & Biol Eng, 2016; 9(6): 84–90.
[20] Cheng X P, Li H W, He J, Wang Q J, Lu C Y, Wang Y B, et al. Optimization of operating parameters of seeding device in plot drill with seeding control system. Int J Agric & Biol Eng, 2021; 14(3): 83–91.
[21] Zhao X S, Guo C L, Sang Y Y, Yu H L, Xu P Y, Du X. Design and orthogonal test of vacuum millet hill-drop seed-metering device. Journal of Agricultural Mechanization Research, 2018; 40(8): 134–140. (in Chinese)
[22] Zhao X S, Yu H L, Ma Y J, Zhang J G, Sang Y Y, Huo X J. Parameter optimization and experiment of negative pressure precision seed-metering device for wheat. Transactions of the CSAE, 2017; 33(11): 11–18. (in Chinese)
[23] Cheng X P, Lu C Y, Meng Z J, Yu, J Y. Design and parameter optimization on wheat precision seed meter with combination of pneumatic and type hole. Transactions of the CSAE, 2018; 34(24): 1–9. (in Chinese)
[24] Liu J X, Wang Q J, Li H W, He J, Lu C Y. Design and seed suction performance of pinhole-tube wheat precision seeding device. Transactions of the CSAE, 2019; 35(11): 10–18. (in Chinese)
[25] Ibrahim E J, Liao Q X, Lei W, Liao Y T, Lu Y. Design and experiment of multi-row pneumatic precision metering device for rapeseed. Int J Agric & Biol Eng, 2018; 11(5): 116–123.
[26] Li S S, Liao Q X, Wang D, Yao L, Lei X L, Wang L, et al. Simulation analyses and experiments of seed filling performance of pneumatic knurled cylinder-type centralized precision metering device for rapeseed. Journal of Huazhong Agricultural University, 2017; 36(5): 99–107. (in Chinese)
[27] Li M, Ding Y C, Liao Q X, Wang X L. Design of loss sowing detection system for rapeseed pneumatic precision metering device. Journal of Shenyang Agricultural University, 2020; 51(2): 185–191. (in Chinese)
[28] China Academy of Agricultural Mechanization Science. Manual for design of agricultural machinery. The first volume. Beijing. China Agricultural Science and Technology Press, 2007. (in Chinese)
[29] Yuan Y. Research of theory and experiment on air suction seed-metering device for direct drilling of rice bud-sowing. Changchun: Jilin University. 2005; 145p. (in Chinese)
[30] Zhao Z, Li Y M, Chen J, Zhou H. Dynamic analysis on seeds pick-up process for vacuum-cylinder seeder. Transactions of the CSAE, 2011; 27(7): 112–116. (in Chinese)
[31] Lei X L, Zhang L, Yang H, Liu Y L, Li Y H, Luo M L. Design and experiment of electric drive control system of precision centralized metering device for rapeseed. Journal of Anhui Agricultural University, 2020; 47(3): 472–479. (in Chinese)
[32] Yu J Y. The design and experimental research on the air-suction roller precision seed-metering device of wheat. Kunming: Kunming University of Science and Technology, 2017; 78p. (in Chinese)